HUMAN GENE THERAPY 20:1–10 (January 2009)

DOI: 10.1089/hum.2008.135

Hydrodynamic Limb Vein Injection of Adeno-Associated Virus Serotype 8 Vector Carrying Canine Myostatin Propeptide Gene into Normal Dogs Enhances Muscle Growth

Chunping Qiao,[1] Juan Li,[1] Hui Zheng,[1,2] Janet Bogan,[3] Jianbin Li,[1] Zhenhua Yuan,[1] Cheng Zhang,[2] Dan Bogan,[3] Joe Kornegay,[3,4] and Xiao Xiao[1,3]

Abstract

Inhibition or blockade of myostatin, a negative growth factor of skeletal muscle, enhances muscle growth and therefore is considered a promising strategy for the treatment of muscle-wasting diseases such as the muscular dystrophies. Previously, we showed that myostatin blockade in both normal and dystrophin-deficient *mdx* mice by systemic delivery of the myostatin propeptide (MPRO) gene by an adeno-associated virus serotype 8 (AAV8) vector could enhance muscle growth and ameliorate dystrophic lesions. Here, we further investigate whether the muscle growth effect of myostatin blockade can be achieved in dogs by gene transfer. First, we cloned the canine MPRO gene, packaged it in the AAV8 vector, and showed robust muscle-enhancing effects after systemic delivery into neonatal mice. This vector was then further tested in two 3-month-old normal dogs (weighing 9.7 and 6.3 kg). The vector was delivered to one limb by hydrodynamic vein injection, and the contralateral limb served as a control. The delivery procedure was safe, without discernible adverse effects. AAV vector DNA and MPRO gene expression were detected by quantitative polymerase chain reaction, Western blotting, and immunofluorescence staining of muscle biopsies. Overexpression of MPRO resulted in enhanced muscle growth without a cytotoxic T lymphocytic immune response, as evidenced by larger myofibers in multiple muscles, increased muscle volume determined by magnetic resonance imaging, and the lack of $CD4^+$ and $CD8^+$ T cell infiltration in the vector-injected limbs. Our preliminary study thus supports further investigation of this therapeutic strategy in the dystrophin-deficient golden retriever muscular dystrophy dog model.

Introduction

Among the genetic muscle degenerative diseases, Duchenne muscular dystrophy (DMD) is the most common and lethal form, afflicting 1 of every 3500 males. DMD is characterized by progressive muscle weakness and degeneration that often leads to severe respiratory or cardiac disease in the patient's late teens and early twenties (Hoffman *et al.*, 1996). DMD is caused by recessive mutations in the dystrophin gene. The absence of functional dystrophin results in loss of the dystrophin-associated protein complex and causes instability of the myofiber plasma membrane (Hoffman *et al.*, 1987; Koenig and Kunkel, 1990). These deficiencies, in turn, lead to chronic muscle damage and degeneration. Because of the lack of an effective treatment, novel therapeutic approaches are being explored (Wang *et al.*, 2000).

Myostatin, also known as growth/differentiation factor-8 (GDF8), is a member of the transforming growth factor (TGF)-β superfamily (McPherron *et al.*, 1997). Numerous studies have demonstrated that myostatin is a negative regulator of skeletal muscle growth. Like other TGF-β family members, myostatin is synthesized as a precursor protein that undergoes proteolytic processing at a dibasic site to generate an N-terminal propeptide, termed myostatin propeptide (MPRO), and a disulfide-linked C-terminal dimer, the biologically active part (for detailed review see Lee, 2004). On cleavage, the mature myostatin C-terminal dimer still remains associated with its inhibitor MPRO in a latent complex. Additional inhibitors of mature myostatin include follistatin (Hill *et al.*, 2002), the follistatin-related gene (FLRG), growth and differentiation factor-associated serum protein-1 (GASP-1) (Hill *et al.*, 2002), and so on. Both myostatin gene knockout mice

[1]Division of Molecular Pharmaceutics, University of North Carolina School of Pharmacy, Chapel Hill, NC 27599.
[2]Department of Neurology, First Affiliated Hospital, Sun Yat-sen University, Guangzhou 510080, China.
[3]Gene Therapy Center, University of North Carolina School of Medicine, Chapel Hill, NC 27599.
[4]Department of Pathology and Laboratory Medicine and Department of Neurology, University of North Carolina School of Medicine, Chapel Hill, NC 27599.

(McPherron *et al.*, 1997; Tobin and Celeste, 2005) and transgenic mice expressing higher levels of myostatin inhibitors (Zhu *et al.*, 2000; Lee and McPherron, 2001) show significant increases in skeletal muscle mass. Furthermore, mutations in the myostatin gene in cattle result in a double-muscling phenotype (McPherron and Lee, 1997). Downregulation of myostatin gene expression in Texel sheep (Clop *et al.*, 2006) caused muscle hypertrophy, as well. In another report, partial loss of myostatin in heterozygous whippet racing dogs resulted in faster running speed, whereas the homozygous whippet dogs were muscular (Mosher *et al.*, 2007). Importantly, a mutation in humans was identified in a healthy child who showed muscle hypertrophy and unusual strength (Schuelke *et al.*, 2004).

The biological function of myostatin has raised the possibility of using inhibitors to promote muscle growth and improve the disease phenotypes in a variety of primary and secondary myopathies, including the muscular dystrophies (Lee, 2004). In a proof-of-principle study, Wagner and coworkers (2002) bred myostatin null mutant mice with *mdx* mice and showed improved muscle regeneration in *mdx* mice lacking myostatin. Administration of a myostatin-blocking antibody increased muscle strength and decreased muscle degeneration in *mdx* mice (Bogdanovich *et al.*, 2002). Similar results were seen when a purified myostatin propeptide was injected (Bogdanovich *et al.*, 2005). Bartoli and coworkers also reported that adeno-associated virus (AAV)-mediated myostatin propeptide ameliorated limb girdle muscular dystrophy in calpain-3-deficient (LGMD2A) mice (Bartoli *et al.*, 2007). Most recently, Wagner's group has shown that inhibition of fibrosis in dystrophic muscle contributes to the benefits of myostatin blockade (Li *et al.*, 2008).

In our previous studies, we have investigated the effect of myostatin inhibition in normal C57BL/6 mice and dystrophin-deficient *mdx* mice by delivering AAV vector encoding the mouse MPRO gene. We observed a significant increase in skeletal muscle mass after systemic delivery of AAV8-MPRO-Ig vector into normal mice (Qiao *et al.*, 2008). In addition, we noticed significantly increased skeletal muscle mass, together with more uniform myofiber size, and less mononuclear cell infiltration and fibrosis after tail vein injection into *mdx* mice (Qiao *et al.*, 2008). Because the small rodent *mdx* mouse model has a mild phenotype and near-normal life span, alternative animal modes have been actively explored. A well-studied large animal model of DMD is the golden retriever muscular dystrophy (GRMD) dog. The GRMD model displays remarkable clinical and pathological similarities to its human homolog (Cooper *et al.*, 1988; Shimatsu *et al.*, 2003, 2005), and has been increasingly used as a large animal model of DMD to evaluate the efficacy of both gene and cell therapy. The current study was designed to test whether the muscle growth-enhancing effect of myostatin blockade could be achieved with a similar strategy in normal dogs, and therefore pave the way for future studies in GRMD dogs.

Materials and Methods

Construction of pAAV-cMPRO-Fc plasmid and AAV vector production

The canine myostatin propeptide (cMPRO) cDNA (gene accession number NM_001002959) was generated by reverse transcription-polymerase chain reaction (PCR) from normal dog muscle tissue. The dog IgG Fc domain (gene accession number AF354264) was also generated by reverse transcription PCR from a dog spleen cDNA library. The forward and reverse primers used for cMPRO were AGCCACCATGCA GAGACTGCAAATCT and tttcatcttctggatctttttggtgtg, respectively. The primers for amplification of the dog IgG Fc domain were dog_IgG_L (cacaccttcccgtccgtcc) and dog_IgG_R (tgcttta tttcatgatgggtgcc). The dog MPRO cDNA and Fc domain were spliced together by the PCR method, and the final product was cloned into an AAV plasmid driven by the chicken β-actin (CAG) promoter including cytomegalovirus (CMV) enhancers and a large synthetic intron (Kootstra *et al.*, 2003). The final constructions were sequenced for verification.

The recombinant viral vector stocks were produced according to the three-plasmid cotransfection method (Xiao *et al.*, 1998). The viral particles were purified twice by CsCl density gradient ultracentrifugation, using the previously published protocol (Qiao *et al.*, 2005). Vector titers, or viral particle numbers, were determined by the DNA dot-blot method and were in the range of 2×10^{12} to 5×10^{12} vector genomes (VG)/ml.

Hydrodynamic limb vein injection of AAV in normal dog limbs

The experimental protocols involving the animals have been approved by the IACUC committee of the University of North Carolina at Chapel Hill (UNC-CH) and are in compliance with all required regulations. Two 3-month-old normal male dogs were used in the hydrodynamic limb vein injection experiments with AAV8-cMPRO-Fc vector. The dogs were first induced by intramuscular administration of atropine sulfate (0.04 mg/kg body weight) and butorphanol tartrate (0.4 mg/kg) and then intubated and maintained with 1–2% sevoflurane. All vital signs were closely monitored throughout the procedure. The limbs to be injected were shaved and scrubbed with Betadine (povidone-iodine) and 70% isopropyl alcohol. A catheter was inserted into the saphenous vein and secured with tape. For pelvic limb injection, a rubber tourniquet was wrapped tightly around the proximal limb at the level of the inguinal area. For thoracic injection, the catheter was placed in the cephalic vein and the tourniquet was wrapped tightly around the proximal limb in the axillary space. The AAV vector dose was 1×10^{13} VG/kg body weight for pelvic limb injection and 3×10^{12} VG/kg body weight for thoracic limb injection. The vector injection volume was 20 ml/kg for the pelvic limb and 12 ml/kg for the thoracic limb. The injection speed was 1 ml/sec for both limbs and was controlled with a syringe pump (model PHD 2000; Harvard Apparatus, Holliston, MA). The total occlusion time was 10 min starting from the beginning of injection. Muscle biopsies of both injected and contralateral limbs were performed 3 months after AAV injection.

Immunofluorescence staining and morphometric analysis

Rat monoclonal anti-laminin β_2-chain antibody (diluted 1:3000; Chemicon/Millipore, Bedford, MA) was used to display the circumferences of the myofibers. Cryo-thin sections of biopsied muscle from treated and control limbs were applied for laminin staining. For morphometric analysis, pictures were taken and the radii of myofibers were analyzed

with MetaMorph software (Molecular Devices, Downingtown, PA), with a minimum of 600 myofibers from each sample.

Real-time PCR analysis

A TaqMan assay was designed for real-time PCR analysis. In brief, the total DNA of muscle tissue was extracted with a QIAamp DNA mini kit (cat. no. 51304; Qiagen, Valencia, CA), and the total RNA was purified with TRIzol reagent (cat. no. 15596-018; Invitrogen, Carlsbad, CA). The reverse transcription reaction was done with a high-capacity cDNA reverse transcription kit (part 4368814; Applied Biosystems, Foster City, CA). The primers and probe for vector DNA-based real-time PCR were as follows: cmv-forward, gta tgt tcc cat agt aac gcc aat ag; cmv-reverse, ggc gta ctt ggc ata tga tac act; cmv probe, FAM-TCA ATG GGT GGA GTA TTT A-MGB. The primers and probe for mRNA quantification were as follows: RT-CAG-F, tct gac tga ccg cgt tac tc; RT-CAG-R, ccg cgg tgg agc tca ag; Cag probe, FAM-TCA ATG GGT GGA GTA TTT A. All the real-time PCRs were performed on a 7300 real-time PCR system (Applied Biosystems) according to the manufacturer's instructions.

Enzyme-linked immunosorbent assay analysis

The enzyme-linked immunosorbent assay (ELISA) method was developed to detect the cMPRO–Fc fusion protein but not the endogenous myostatin propeptide. First, a clear 96-well plate was coated with anti-mouse antibody (diluted 1:500) overnight at 4°C. Second, the plate was incubated with anti-dog MPRO polyclonal antibody (diluted 1:1000; generated from mice by the laboratory of X. Xiao, UNC-CH) for 0.5 hr at room temperature. We did not directly coat the plate with the anti-dog MPRO antibody because this antibody was unpurified; coating unpurified protein would induce undesired high background. Third, the plate was blocked with 1% milk for 2–6 hr at room temperature. The fourth step was to incubate with antigen (tissue or sera containing MPRO–Fc, or purified cMPRO–Fc protein from plasmid-transfected conditional medium). The plate was then incubated with anti-dog Fc–horseradish peroxidase (HRP) conjugate (cat. no. 30371, diluted 1:20,000; Alpha Diagnostic International, San Antonio, TX) followed by color development. In the data analysis part, the optical density (OD) readings from tissues and sera were blanked with normal uninjected dog muscle tissue and normal uninjected dog serum, respectively. The ELISA ensemble kit was purchased from Alpha Diagnostic International.

Magnetic resonance imaging analysis

Magnetic resonance imaging (MRI) studies were done with a Siemens 3-T Allegra head-only system (Siemens Medical Solutions, Malvern, PA) at the UNC-CH Animal Imaging Center. T2-weighted images with and without fat saturation were completed. Proximal and distal limbs were imaged separately. Image analysis was done through the UNC-CH Neuro Image Analysis Laboratory, using the software program ITK-SNAP (www.itksnap.org).[1] We completed region-of-interest volumetric quantitative measurements of the muscle cross-sectional area (mm^3) in both pelvic limbs from each dog at the level of the mid-femur and the proximal and distal tibia (see Fig. 4c). A total of five consecutive 1-mm images were segmented. The measurements varied among the different levels and muscles, with no consistent differences (Yushkevich *et al.*, 2006).

Results

Test of biological function of AAV8-cMPRO-Fc vector in mice

To avoid an immune response against the mouse MPRO–Fc in dogs, we cloned canine myostatin propeptide cDNA by PCR and fused it with the canine IgG Fc domain to prolong its half-life *in vivo* (see Materials and Methods for details) (Wolfman *et al.*, 2003; Qiao *et al.*, 2008). Similar to our previous study, we used a CAG promoter (consisting of the CMV enhancer, chicken β-actin promoter, and a globin intron) to drive the myostatin propeptide gene for robust and long-term expression *in vivo* (Qiao *et al.*, 2008). Before performing experiments in dogs, we tested whether the cMPRO–Fc vector is functional in mice. AAV8-cMPRO-Fc vector was delivered into neonatal ICR mice by intraperitoneal injection to minimize humoral immune responses to the dog protein. The AAV-treated mice and untreated littermates were weighed periodically for body weight gain. As shown in Fig. 1a, the treated mice had significant weight gain (22.7 ± 1.16 g for females) over the untreated littermates (20.4 ± 0.49 g for females) at 4 weeks, when the mice were weaned. At 7 weeks of age, the average body weight of treated mice (33.7 ± 2.3 g for females) increased by more than 30% over the untreated littermates (27 ± 1.5 g for females). The AAV8-cMPRO-Fc vector-treated mice also appeared heavier and more muscular (Fig. 1b). Histological examination revealed that muscle fiber sizes of treated mice were essentially doubled (Fig. 1c). These data clearly indicated that the AAV-cMPRO-Fc vector was functional in mice.

Detection of vector DNA and MPRO–Fc mRNA expression in dog limbs after hydrodynamic limb vein injection

We next proceeded to the experiments in dogs. To deliver the AAV vector into multiple muscles, we used the hydrodynamic limb vein (HLV) delivery method, which rapidly delivers a solution containing nucleic acids or viral vectors into a limb that is blocked by a tourniquet during injection (Arruda *et al.*, 2005; Herweijer and Wolff, 2007). We chose to use AAV8 as the vector, because it is able to cross blood vessel barriers and transduce skeletal muscles efficiently via systemic delivery (Wang *et al.*, 2005). Two normal dogs were used in this study. Dog Ramone (6.3 kg) had the AAV vector injected in the pelvic limb, whereas dog Link (9.7 kg) had the vector injected in the thoracic limb, both by the HLV injection method. The AAV8-cMPRO-Fc vector dose was 1×10^{13} VG/kg body weight for Ramone, and 3×10^{12} VG/kg body weight for Link. A lower vector dose was used in Link because of the smaller size of the thoracic versus pelvic limbs. A rubber tourniquet was used to block venous return at the level of the inguinal and axillary areas for 10 min during vector injection. No procedure- or vector-related adverse events were observed during or after vector injection.

Three months after vector delivery, biopsy was performed on various muscles of both injected limbs and the

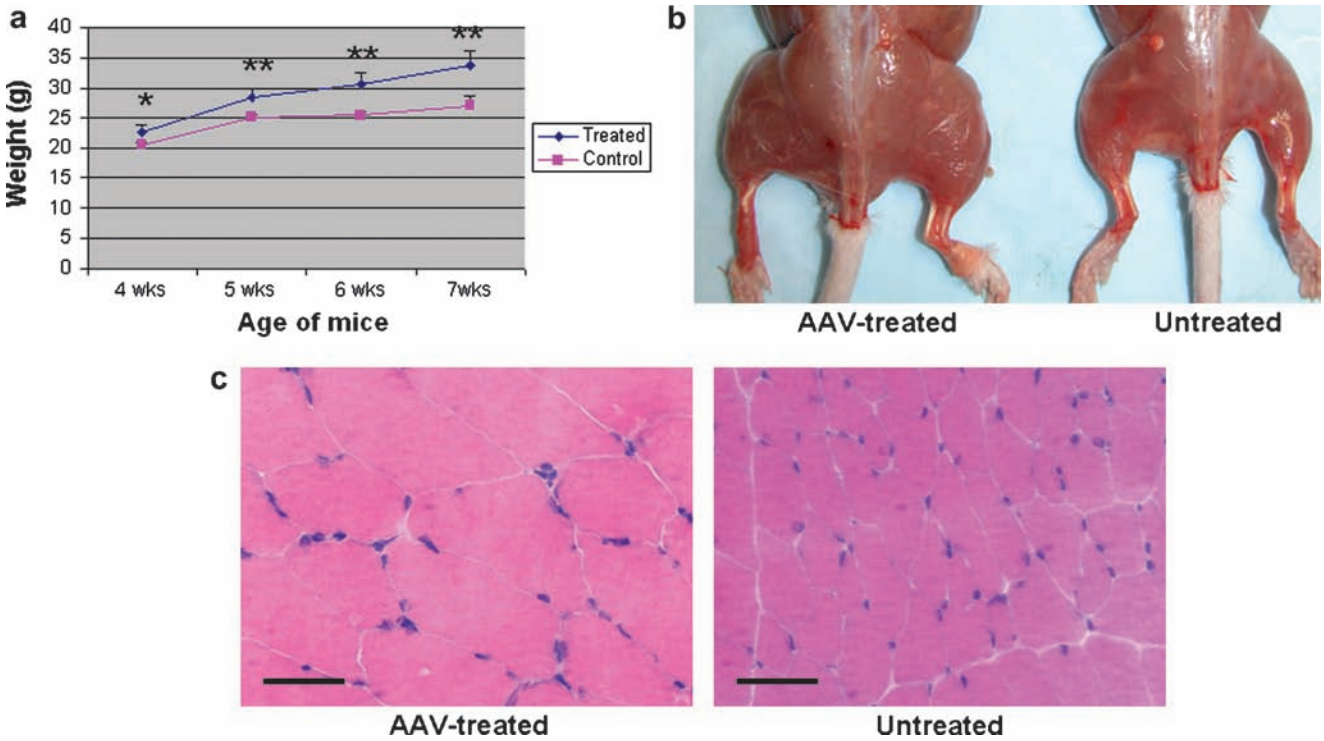

FIG. 1. Muscle growth-enhancing effects of AAV-cMPRO-Fc in mice. The AAV8-cMPRO-Fc vector was delivered into neonatal ICR mice by intraperitoneal injection. There were seven mice for each group. (**a**) Growth curve of the mice. $^{*}p < 0.05$; $^{**}p < 0.01$. (**b**) Photograph of skinned AAV8-cMPRO-Fc-treated mouse versus control mouse. The mice were 7 weeks old when the picture was taken. Note that the treated mouse is more muscular than the control. (**c**) Hematoxylin and eosin (H&E) staining of treated versus control quadriceps muscle. Both pictures were taken at the same magnification. Treated muscle fiber appeared bigger compared with control muscle fiber. Scale bars: 100 μm.

contralateral control limbs. Quantitative PCR of total DNA from each muscle biopsy showed that AAV vector copy numbers (CAG promoter as the target sequence) in the injected pelvic limb of dog Ramone were consistently higher than in the uninjected contralateral pelvic limb in all five pairs of biopsy samples (Fig. 2a). However, the copy numbers on a per-diploid genome basis (or per nucleus for muscle myofibers) were not high. Specifically, the gastrocnemius (lower limb) and vastus lateralis and biceps femoris (upper limb) muscles had 1.2 to 1.55 copies per nucleus, whereas the long digital extensor (lower limb) and cranial sartorius (upper limb) had 0.08 to 0.25 copy per nucleus (Fig. 2a). cMPRO–Fc mRNA expression was determined by quantitative real-time (RT)-PCR. The profiles were in general agreement with the vector DNA copy numbers. Thus, higher mRNA levels were found in muscle samples with higher vector DNA copy numbers (Fig. 2b). Because quantitative RT-PCR detected the chicken β-globin exon–intron sequence, a part of the CAG promoter in the cMPRO–Fc expression cassette, the data reflected only the levels of cMPRO mRNA derived from the vector DNA, not from the endogenous cMPRO gene. The lower RT-PCR signals detected in the contralateral muscles might have resulted from cMPRO–Fc vector that disseminated systemically from the injected limb.

Detection of cMPRO–Fc protein in injected muscles and sera

We next wished to confirm vector gene expression by examining the cMPRO–Fc protein product in muscle and sera. Western blotting of muscle biopsy samples from Ramone showed cMPRO–Fc of the expected molecular weight in the AAV-treated limb (Fig. 3a) in the three muscles that had higher vector DNA copy numbers and mRNA levels (Fig. 2a and b). The presence of cMPRO–Fc protein was also confirmed by immunofluorescence staining of gastrocnemius and other muscles (Fig. 3b). Furthermore, quantitative ELISA analysis of serum samples detected cMPRO–Fc protein in dog Ramone as early as 1 week after vector injection and the concentration slightly declined over the course of 4 weeks (Fig. 3c). The serum cMPRO–Fc levels were, however, more than an order of magnitude lower than those of muscle (data not shown). Together, the preceding data showed that cMPRO–Fc gene expression was successfully achieved in multiple muscles after HLV injection.

Enhanced muscle growth resulting from cMPRO–Fc expression

Earlier in this study, we observed an increase in muscle myofiber size by overexpression of cMPRO–Fc in mice. Here, we wished to determine whether cMPRO–Fc expression could also enhance growth of dog muscles. Hematoxylin and eosin (H&E) staining was performed on the AAV-treated and untreated limbs to determine myofiber sizes. The myofiber diameters of gastrocnemius and biceps femoris muscles of dog Ramone showed the most significant increases in treated limb relative to untreated limb (Fig. 3a). This was further confirmed by quantitative analysis of a large number of myofibers by digital morphometric analyses

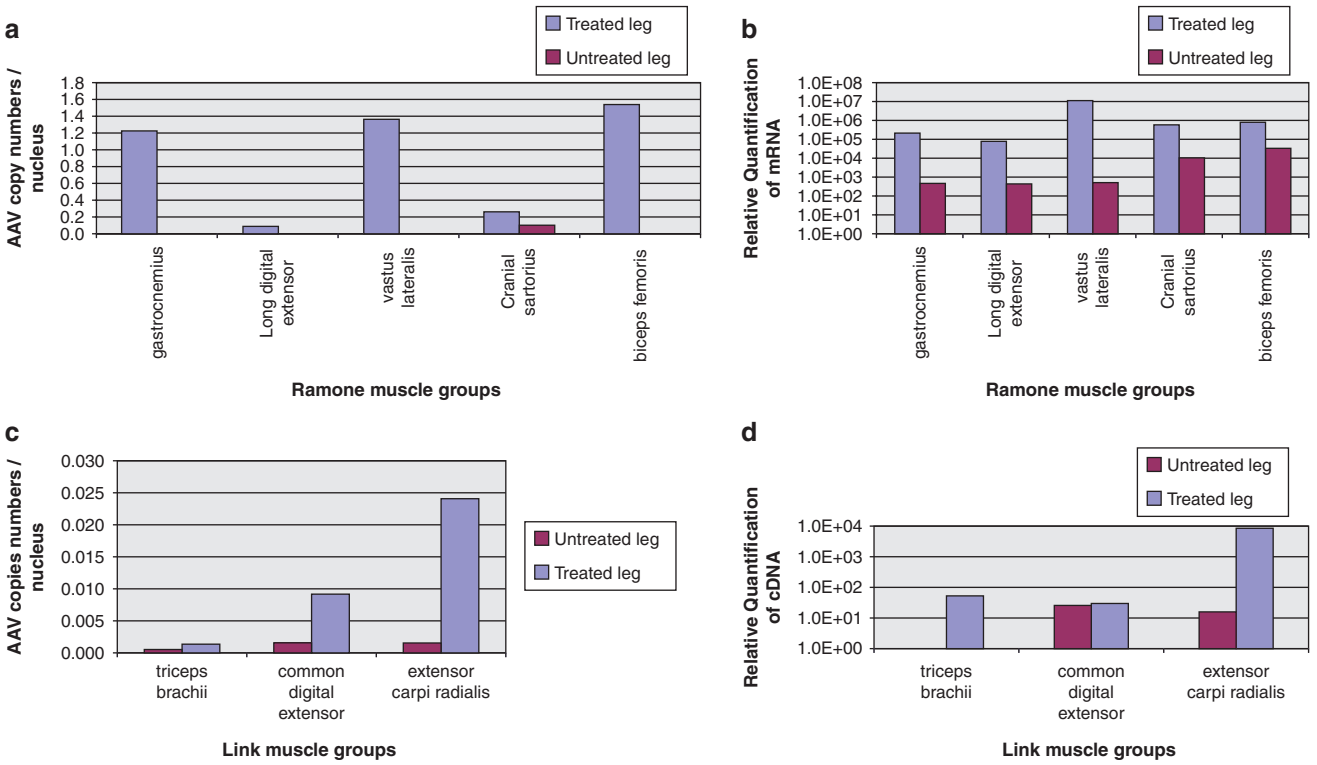

FIG. 2. Real-time PCR analysis of vector DNA and transgene mRNA. Three months after vector delivery, biopsy was performed on treated and control legs. (**a**) Real-time PCR analysis for vector DNA copy numbers in dog Ramone. AAV8-cMPRO-Fc vectors were most numerous in skeletal muscle from treated leg (blue columns), but some were present in control leg muscle (red columns). (**b**) Real-time PCR for quantification of cMPRO mRNA in dog Ramone. There is a 100- to 10,000-fold difference in transgene expression in mRNA level between treated (blue columns) and control legs (red columns). (**c**) Real-time PCR assay for vector DNA copy numbers in dog Link. Red columns, control leg data; blue columns, treated leg data. (**d**) Real-time PCR for cMPRO cDNA quantification of dog Link.

(Fig. 3b). However, the myofiber sizes in the remaining three muscles including vastus lateralis, which had good expression of the cMPRO–Fc gene, did not show significant differences between vector-treated and untreated limbs (Fig. 3b). The reason remains unclear and is discussed later. We also examined the myofiber sizes of biopsies taken from dog Link, who received vector injection via a thoracic limb. Only the extensor carpi radialis muscle showed significant myofiber size increase in the vector-treated limb (Fig. 4a). This muscle also had a higher vector DNA copy number and higher cMPRO mRNA level than the other two muscle groups, the triceps brachii and common digital extensor (Fig. 2c and d). This result is consistent with the degree of transgene expression.

Finally, we performed MRI on perfused versus nonperfused limbs of dog Ramone to examine whether muscle volume was enlarged after vector delivery. Similar to the results obtained in morphometric analyses, we observed muscle volume increase in some muscles, but not in all the muscles. For example, muscle volume in the mid-femur segment of the vector-perfused limb was slightly higher than that of the nonperfused limb (27,061 vs. 25,380 mm^3) (Fig. 4c). In the tibia middle segment, the muscle volume of the perfused limb was also slightly increased compared with that of the nonperfused limb ((3051 vs. 2653 mm^3) (Fig. 4c). However, in the tibia proximal segment, there was no difference in muscle volume between the perfused limb and nonperfused limb (6190 vs. 6112 mm^3) (Fig. 4c).

Discussion

Inhibition or blockade of myostatin to promote muscle growth has been explored as a potential treatment for muscle-wasting diseases, including sarcopenia, cachexia, and muscular dystrophies (Bogdanovich *et al.*, 2002, 2005; Lee *et al.*, 2005; Tobin and Celeste, 2005; Ohsawa *et al.*, 2006; Bartoli *et al.*, 2007; Wagner *et al.*, 2008). Here, we investigated the muscle growth effect of myostatin inhibition by gene delivery of a natural inhibitor of myostatin, the myostatin propeptide, in normal dogs. To achieve broad transgene expression in the limb muscles, the hydrodynamic limb vein perfusion technique and AAV8 vector were used. We have shown the first evidence that somatic gene transfer of cMPRO–Fc gene in dogs can enhance growth in multiple muscle groups, as evidenced by increased myofiber sizes, similar to the results obtained in previous mouse studies (Qiao *et al.*, 2008). No vector-related adverse effects, including cellular immune responses after gene transfer, were observed. This study supports future investigation of this therapeutic strategy in dystrophin-deficient dogs.

Although cMPRO–Fc expression enhanced growth of multiple muscles, not all the muscles that expressed cMPRO–Fc

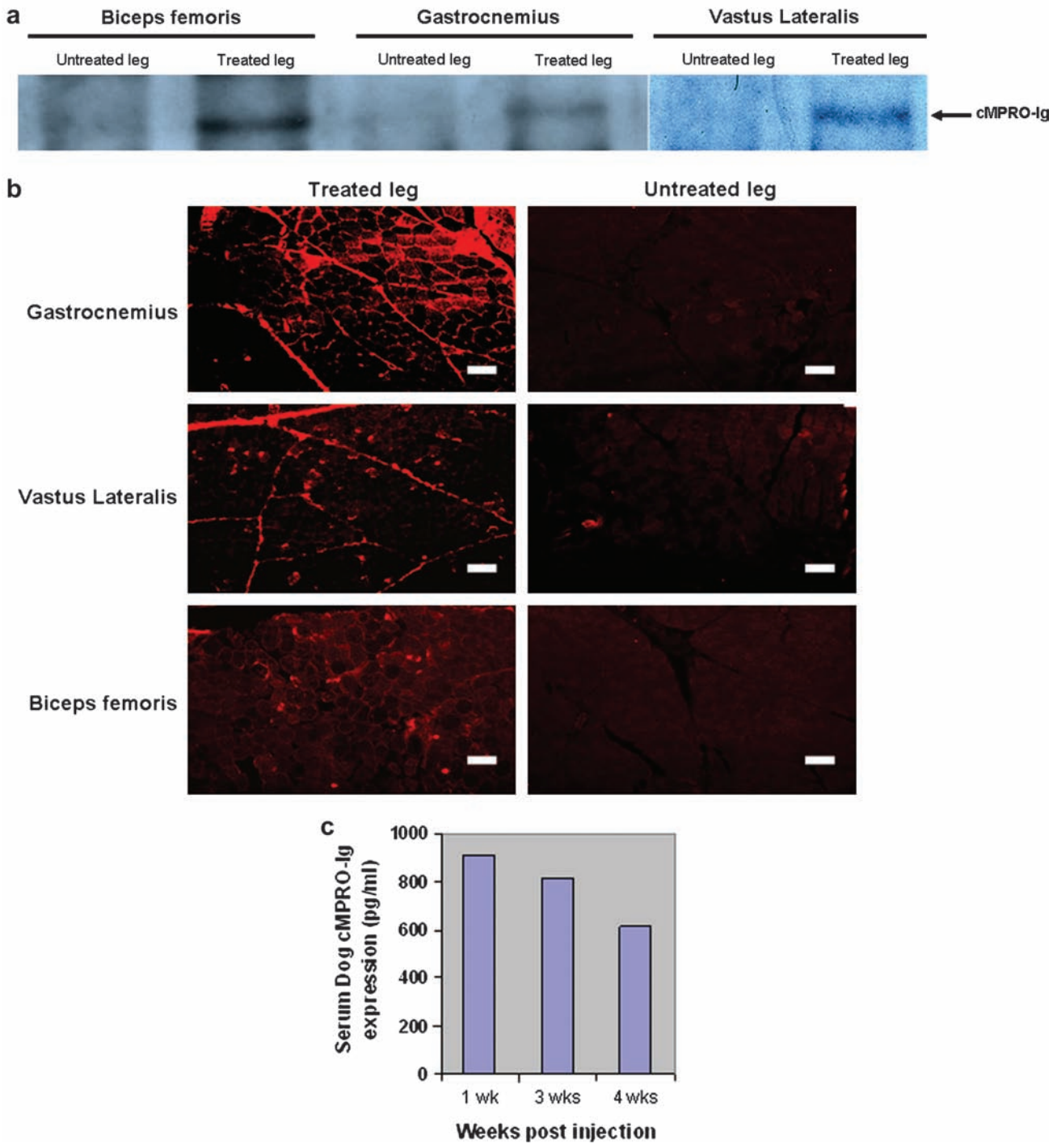

FIG. 3. Detection of cMPRO–Fc protein expression. (**a**) Western blot analysis demonstrates the expected band from the treated muscles of dog Ramone. (**b**) Immunofluorescence staining against dog MPRO indicates that cMPRO–Fc is expressed in treated muscle. Scale bar: 100 μm. (**c**) ELISA analysis of injected dog (Ramone) serum. cMPRO–Fc was detected from serum 1 week after vector delivery (900 pg/ml). Four weeks after vector delivery, the expression serum level of cMPRO–Fc in Ramone was reduced to about 600 pg/ml.

showed myofiber size increase. A plausible explanation is that the relatively low vector copy numbers in those muscles may have produced insufficient gene expression. The vector doses in the dogs were more than 10 times lower than in mice, if the doses were based on the weight of targeted tissues (5×10^{11} VG/neonatal mouse was approximately 5×10^{14} VG/kg body weight; whereas the vector dose in the dogs was no more than 10^{13} VG/kg body weight). Quantitative vector DNA PCR results showed that the highest vector copy number in the AAV-injected dog limbs was 1.55 copies per nucleus. On the other hand, vector copy numbers in some muscles were as low as <0.1 copy per nucleus; the vector copy

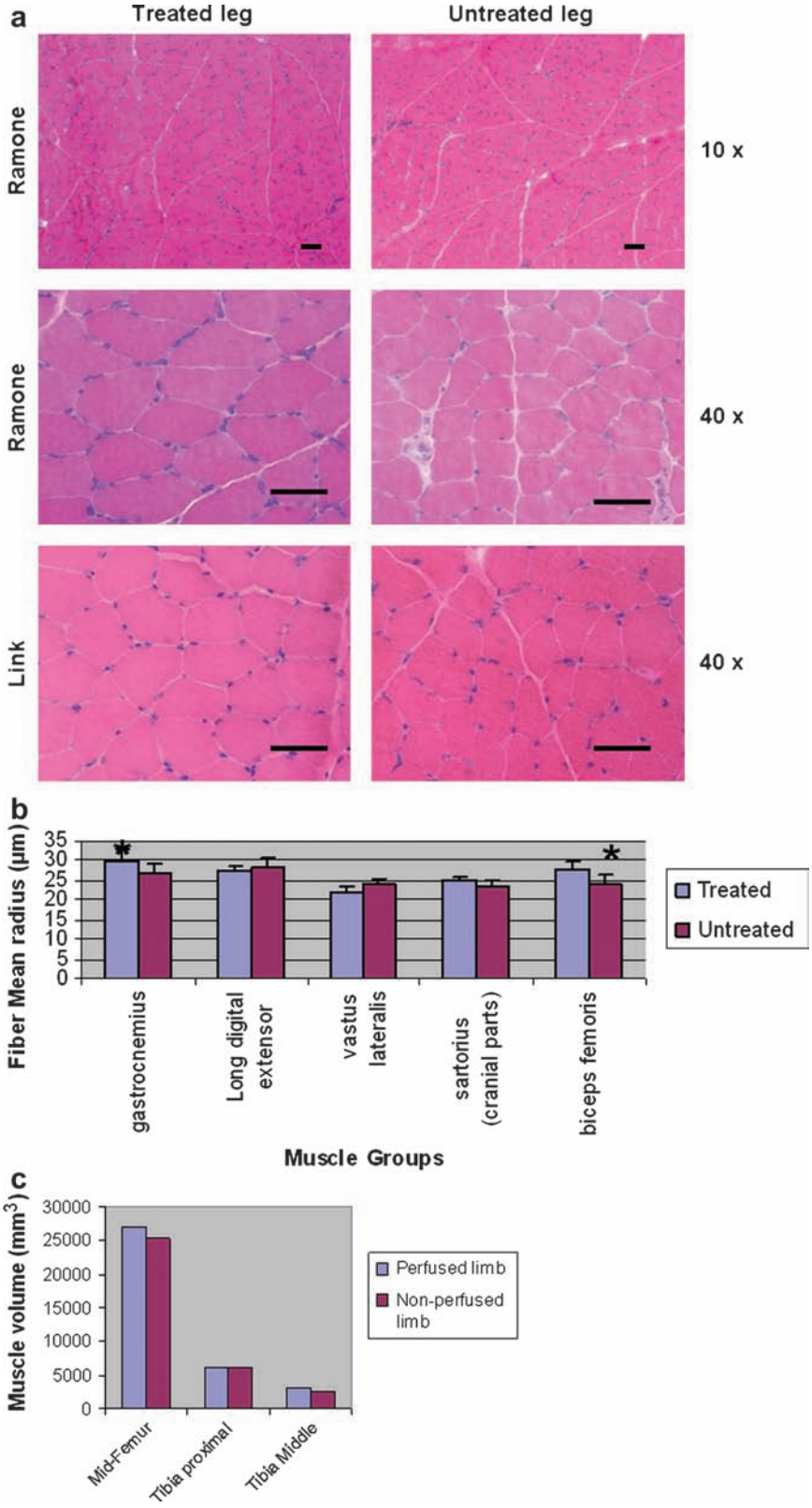

FIG. 4. Enhancement of muscle growth by AAV8-cMPRO-Fc in injected dog hind limbs. (**a**) Histological examination of muscle sections. It is notable that treated muscle displayed larger muscle fiber sizes without mononuclear cell infiltration. Scale bars: 100 μm. (**b**) Semiquantitative analysis of muscle fiber sizes, using MetaMorph software. In detail, 8- to 10-μm cryo-thin sections of biopsied muscles (from dog Ramone) were subjected to immunofluorescence staining against the laminin γ chain to display circumferences of the myofibers. Pictures were taken and radii of the myofibers were analyzed with MetaMorph software, using a minimum of 300 myofibers from each muscle. (**c**) MRI volumetric analysis indicated that muscle sizes were increased in some muscles of the vector-perfused leg, compared with the contralateral nonperfused control leg. Data were obtained from five consecutive 1-mm cross-section segments.

numbers in skeletal muscles of adult mice were in the neighborhood of 10 copies per nucleus after neonatal AAV8 injection (Wang *et al.*, 2005). This could account, in part, for the less robust enhancement of muscle growth in dogs than in mice. Apparently, room exists for technical improvement, such as better injection techniques, higher vector doses, and choice of more efficient AAV serotypes. Indeed, AAV9 vector has been shown to be more robust than AAV8 in both small and large animals in systemic delivery (Inagaki *et al.*, 2006; Pacak *et al.*, 2006). Preliminary data of Duan and coworkers

(Yue *et al.*, 2008) and our own data obtained in dogs support this notion. As mentioned in Results, we did not detect myofiber size increase in the vastus lateralis muscle of dog Ramone, although vector DNA copy number, mRNA, and cMPRO–Fc protein expression were similar in this muscle as in the gastrocnemius and biceps femoris muscles, both of which showed growth enhancement. The weaker growth enhancement in certain muscles might be due to a higher threshold for myostatin inhibition in those muscle groups, although this phenomenon was not apparent in mice. Interestingly, homozygous myostatin gene mutant whippet dogs are more muscular than their heterozygous littermates (Mosher *et al.*, 2007). This indicates that growth enhancement through myostatin inhibition in dogs is dose dependent, as in mice. It remains to be investigated whether in dogs the dystrophic muscles are also more responsive than the normal muscles to myostatin inhibition as seen in our previous mouse studies (Qiao *et al.*, 2008).

We did not observe significant $CD4^+$ or $CD8^+$ T lymphocyte infiltration in AAV8-cMPRO-Fc-treated skeletal muscles in this study. For example, the total $CD4^+$ T cells in an entire cross-sectional area of a muscle biopsy were less than 20 as revealed by immunofluorescence staining (data not shown). In contrast, Wang and coworkers reported that strong cellular immune responses appeared on AAV2 and AAV6 vector delivery into skeletal muscles of normal dogs (Wang *et al.*, 2007). Their study differed from ours in several ways, such as in delivery route, AAV serotypes used, as well as transgenes expressed. We believe those factors will affect the immune response in dogs after delivery of AAV vector into skeletal muscles, as other groups have also achieved successful transgene expression and therapeutic effect in dogs without immunosuppressant drugs (Jiang *et al.*, 2006; Koeberl *et al.*, 2008).

Dystrophin-deficient GRMD dogs show signs of pathology similar to those of DMD patients and serve as a useful and clinically relevant large animal model (Schatzberg *et al.*, 1998; Liu *et al.*, 2004). Two of the major pathological hallmarks of GRMD are muscle atrophy and fibrosis. Blockade of myostatin could counter both by enhancing muscle growth and inhibiting fibrosis (Li *et al.*, 2008). There are several venues to evaluate the therapeutic effects of myostatin blockade/inhibition in GRMD dogs. One of them is the frequent administration of a purified myostatin-blocking antibody. A humanized antibody, MYO-029, has been used in clinical trials and has shown safety (Wagner *et al.*, 2008). However, at present there is no caninized antibody available for studies in dogs. Another way to test efficacy is to cross the GRMD dogs with myostatin mutant whippet dogs (Mosher *et al.*, 2007), which show muscle hypertrophy. However, it will be time-consuming to cross the two breeds. In addition, the influence of myostatin mutation in this case will exert its effects from the embryonic stage, which is not possible in a clinical setting for DMD therapy. As a result, somatic gene delivery of myostatin blockers or inhibitors in the GRMD dog remains a viable and practical approach and, if successful, could be translated into human clinical trials. In fact, several reports, including ours, have shown that myostatin blockade is effective in ameliorating dystrophic pathology in *mdx* mice (Bogdanovich *et al.*, 2002, 2005; Wagner *et al.*, 2002; Haidet *et al.*, 2008; Nakatani *et al.*, 2008; Qiao *et al.*, 2008). Further study in large animal models, such as GRMD dogs, is well warranted.

Acknowledgments

This work was supported by NIH grants U24NS059696 to J.K. and U54AR050733 to J.K. and X.X., and by a China Scholarship Council predoctoral fellowship to H.Z.

Author Disclosure Statement

No competing financial interests exist.

References

Arruda, V.R., Stedman, H.H., Nichols, T.C., Haskins, M.E., Nicholson, M., Herzog, R.W., Couto, L.B., and High, K.A. (2005). Regional intravascular delivery of AAV-2-F.IX to skeletal muscle achieves long-term correction of hemophilia B in a large animal model. Blood 105, 3458–3464.

Bartoli, M., Poupiot, J., Vulin, A., Fougerousse, F., Arandel, L., Daniele, N., Roudaut, C., Noulet, F., Garcia, L., Danos, O., and Richard, I. (2007). AAV-mediated delivery of a mutated myostatin propeptide ameliorates calpain 3 but not α-sarcoglycan deficiency. Gene Ther. 14, 733–740.

Bogdanovich, S., Krag, T.O., Barton, E.R., Morris, L.D., Whittemore, L.A., Ahima, R.S., and Khurana, T.S. (2002). Functional improvement of dystrophic muscle by myostatin blockade. Nature 420, 418–421.

Bogdanovich, S., Perkins, K.J., Krag, T.O., Whittemore, L.A., and Khurana, T.S. (2005). Myostatin propeptide-mediated amelioration of dystrophic pathophysiology. FASEB J. 19, 543–549.

Clop, A., Marcq, F., Takeda, H., Pirottin, D., Tordoir, X., Bibe, B., Bouix, J., Caiment, F., Elsen, J.M., Eychenne, F., Larzul, C., Laville, E., Meish, F., Milenkovic, D., Tobin, J., Charlier, C., and Georges, M. (2006). A mutation creating a potential illegitimate microRNA target site in the myostatin gene affects muscularity in sheep. Nat. Genet. 38, 813–818.

Cooper, B.J., Winand, N.J., Stedman, H., Valentine, B.A., Hoffman, E.P., Kunkel, L.M., Scott, M.O., Fischbeck, K.H., Kornegay, J.N., Avery, R.J., Williams, J.R., Schmickel, R.D., and Sylvester, J.E. (1988). The homologue of the Duchenne locus is defective in X-linked muscular dystrophy of dogs. Nature 334, 154–156.

Haidet, A.M., Rizo, L., Handy, C., Umapathi, P., Eagle, A., Shilling, C., Boue, D., Martin, P.T., Sahenk, Z., Mendell, J.R., and Kaspar, B.K. (2008). Long-term enhancement of skeletal muscle mass and strength by single gene administration of myostatin inhibitors. Proc. Natl. Acad. Sci. U.S.A. 105, 4318–4322.

Herweijer, H., and Wolff, J.A. (2007). Gene therapy progress and prospects: Hydrodynamic gene delivery. Gene Ther. 14, 99–107.

Hill, J.J., Davies, M.V., Pearson, A.A., Wang, J.H., Hewick, R.M., Wolfman, N.M., and Qiu, Y. (2002). The myostatin propeptide and the follistatin-related gene are inhibitory binding proteins of myostatin in normal serum. J. Biol. Chem. 277, 40735–40741.

Hoffman, E.P., Brown, R.H., JR., and Kunkel, L.M. (1987). Dystrophin: The protein product of the Duchenne muscular dystrophy locus. Cell 51, 919–928.

Hoffman, E.P., Pegoraro, E., Scacheri, P., Burns, R.G., Taber, J.W., Weiss, L., Spiro, A., and Blattner, P. (1996). Genetic counseling of isolated carriers of Duchenne muscular dystrophy. Am. J. Med. Genet. 63, 573–580.

Inagaki, K., Fuess, S., Storm, T.A., Gibson, G.A., McTiernan, C.F., Kay, M.A., and Nakai, H. (2006). Robust systemic transduction with AAV9 vectors in mice: Efficient global car-

diac gene transfer superior to that of AAV8. Mol. Ther. 14, 45–53.

Jiang, H., Lillicrap, D., Patarroyo-White, S., Liu, T., Qian, X., Scallan, C.D., Powell, S., Keller, T., McMurray, M., Labelle, A., Nagy, D., Vargas, J.A., Zhou, S., Couto, L.B., and Pierce, G.F. (2006). Multiyear therapeutic benefit of AAV serotypes 2, 6, and 8 delivering factor VIII to hemophilia A mice and dogs. Blood 108, 107–115.

Koeberl, D.D., Pinto, C., Sun, B., Li, S., Kozink, D.M., Benjamin, D.K., JR., Demaster, A.K., Kruse, M.A., Vaughn, V., Hillman, S., Bird, A., Jackson, M., Brown, T., Kishnani, P.S., and Chen, Y.T. (2008). AAV vector-mediated reversal of hypoglycemia in canine and murine glycogen storage disease type Ia. Mol. Ther. 16, 665–672.

Koenig, M., and Kunkel, L.M. (1990). Detailed analysis of the repeat domain of dystrophin reveals four potential hinge segments that may confer flexibility. J. Biol. Chem. 265, 4560–4566.

Kootstra, N.A., Matsumura, R., and Verma, I.M. (2003). Efficient production of human FVIII in hemophilic mice using lentiviral vectors. Mol. Ther. 7, 623–631.

Lee, S.J. (2004). Regulation of muscle mass by myostatin. Annu. Rev. Cell Dev. Biol. 20, 61–86.

Lee, S.J., and McPherron, A.C. (2001). Regulation of myostatin activity and muscle growth. Proc. Natl. Acad. Sci. U.S.A. 98, 9306–9311.

Lee, S.J., Reed, L.A., Davies, M.V., Girgenrath, S., Goad, M.E., Tomkinson, K.N., Wright, J.F., Barker, C., Ehrmantraut, G., Holmstrom, J., Trowell, B., Gertz, B., Jiang, M.S., Sebald, S.M., Matzuk, M., Li, E., Liang, L.F., Quattlebaum, E., Stotish, R.L., and Wolfman, N.M. (2005). Regulation of muscle growth by multiple ligands signaling through activin type II receptors. Proc. Natl. Acad. Sci. U.S.A. 102, 18117–18122.

Li, Z.B., Kollias, H.D., and Wagner, K.R. (2008). Myostatin directly regulates skeletal muscle fibrosis. J. Biol. Chem. 283, 19371–19378.

Liu, J.M., Okamura, C.S., Bogan, D.J., Bogan, J.R., Childers, M.K., and Kornegay, J.N. (2004). Effects of prednisone in canine muscular dystrophy. Muscle Nerve 30, 767–773.

McPherron, A.C., and Lee, S.J. (1997). Double muscling in cattle due to mutations in the myostatin gene. Proc. Natl. Acad. Sci. U.S.A. 94, 12457–12461.

McPherron, A.C., Lawler, A.M., and Lee, S.J. (1997). Regulation of skeletal muscle mass in mice by a new TGF-β superfamily member. Nature 387, 83–90.

Mosher, D.S., Quignon, P., Bustamante, C.D., Sutter, N.B., Mellersh, C.S., Parker, H.G., and Ostrander, E.A. (2007). A mutation in the myostatin gene increases muscle mass and enhances racing performance in heterozygote dogs. PLoS Genet. 3, e79.

Nakatani, M., Takehara, Y., Sugino, H., Matsumoto, M., Hashimoto, O., Hasegawa, Y., Murakami, T., Uezumi, A., Takeda, S., Noji, S., Sunada, Y., and Tsuchida, K. (2008). Transgenic expression of a myostatin inhibitor derived from follistatin increases skeletal muscle mass and ameliorates dystrophic pathology in *mdx* mice. FASEB J. 22, 477–487.

Ohsawa, Y., Hagiwara, H., Nakatani, M., Yasue, A., Moriyama, K., Murakami, T., Tsuchida, K., Noji, S., and Sunada, Y. (2006). Muscular atrophy of caveolin-3-deficient mice is rescued by myostatin inhibition. J. Clin. Invest. 116, 2924–2934.

Pacak, C.A., Mah, C., Thattaliyath, B., Conlon, T., Lewis, M., Cloutier, D.E., Zolotukhin, I., Tarantal, A., and Byrne, B.J. (2006). Recombinant adeno-associated virus serotype 9 leads to preferential cardiac transduction *in vivo*. Circ. Res. 99, e3–e9.

Qiao, C., Li, J., Zhu, T., Draviam, R., Watkins, S., Ye, X., Chen, C., Li, J., and Xiao, X. (2005). Amelioration of laminin-α_2-deficient congenital muscular dystrophy by somatic gene transfer of miniagrin. Proc. Natl. Acad. Sci. U.S.A. 102, 11999–12004.

Qiao, C., Li, J., Jiang, J., Zhu, X., Wang, B., Li, J., and Xiao, X. (2008). Myostatin propeptide gene delivery by adeno-associated virus serotype 8 vectors enhances muscle growth and ameliorates dystrophic phenotypes in *mdx* mice. Hum. Gene Ther. 19, 241–254.

Schatzberg, S.J., Anderson, L.V., Wilton, S.D., Kornegay, J.N., Mann, C.J., Solomon, G.G., and Sharp, N.J. (1998). Alternative dystrophin gene transcripts in golden retriever muscular dystrophy. Muscle Nerve 21, 991–998.

Schuelke, M., Wagner, K.R., Stolz, L.E., Hubner, C., Riebel, T., Komen, W., Braun, T., Tobin, J.F., and Lee, S.J. (2004). Myostatin mutation associated with gross muscle hypertrophy in a child. N. Engl. J. Med. 350, 2682–2688.

Shimatsu, Y., Katagiri, K., Furuta, T., Nakura, M., Tanioka, Y., Yuasa, K., Tomohiro, M., Kornegay, J.N., Nonaka, I., and Takeda, S. (2003). Canine X-linked muscular dystrophy in Japan (CXMDJ). Exp. Anim. 52, 93–97.

Shimatsu, Y., Yoshimura, M., Yuasa, K., Urasawa, N., Tomohiro, M., Nakura, M., Tanigawa, M., Nakamura, A., and Takeda, S. (2005). Major clinical and histopathological characteristics of canine X-linked muscular dystrophy in Japan, CXMDJ. Acta Myol. 24, 145–154.

Tobin, J.F., and Celeste, A.J. (2005). Myostatin, a negative regulator of muscle mass: Implications for muscle degenerative diseases. Curr. Opin. Pharmacol. 5, 328–332.

Wagner, K.R., McPherron, A.C., Winik, N., and Lee, S.J. (2002). Loss of myostatin attenuates severity of muscular dystrophy in *mdx* mice. Ann. Neurol. 52, 832–836.

Wagner, K.R., Fleckenstein, J.L., Amato, A.A., Barohn, R.J., Bushby, K., Escolar, D.M., Flanigan, K.M., Pestronk, A., Tawil, R., Wolfe, G.I., Eagle, M., Florence, J.M., King, W.M., Pandya, S., Straub, V., Juneau, P., Meyers, K., Csimma, C., Araujo, T., Allen, R., Parsons, S.A., Wozney, J.M., Lavallie, E.R., and Mendell, J.R. (2008). A phase I/II trial of MYO-029 in adult subjects with muscular dystrophy. Ann. Neurol. 63, 561–571.

Wang, B., Li, J., and Xiao, X. (2000). Adeno-associated virus vector carrying human minidystrophin genes effectively ameliorates muscular dystrophy in *mdx* mouse model. Proc. Natl. Acad. Sci. U.S.A. 97, 13714–13719.

Wang, Z., Zhu, T., Qiao, C., Zhou, L., Wang, B., Zhang, J., Chen, C., Li, J., and Xiao, X. (2005). Adeno-associated virus serotype 8 efficiently delivers genes to muscle and heart. Nat. Biotechnol. 23, 321–328.

Wang, Z., Allen, J.M., Riddell, S.R., Gregorevic, P., Storb, R., Tapscott, S.J., Chamberlain, J.S., and Kuhr, C.S. (2007). Immunity to adeno-associated virus-mediated gene transfer in a random-bred canine model of Duchenne muscular dystrophy. Hum. Gene Ther. 18, 18–26.

Wolfman, N.M., McPherron, A.C., Pappano, W.N., Davies, M.V., Song, K., Tomkinson, K.N., Wright, J.F., Zhao, L., Sebald, S.M., Greenspan, D.S., and Lee, S.J. (2003). Activation of latent myostatin by the BMP-1/tolloid family of metalloproteinases. Proc. Natl. Acad. Sci. U.S.A. 100, 15842–15846.

Xiao, X., Li, J., and Samulski, R.J. (1998). Production of high-titer recombinant adeno-associated virus vectors in the absence of helper adenovirus. J. Virol. 72, 2224–2232.

Yue, Y., Ghosh, A., Long, C., Bostick, B., Smith, B.F., Kornegay, J.N., and Duan, D. (2008). Systemic AAV-9 delivery in normal dog leads to high-level persistent transduction in whole body skeletal muscle. Presented at the 11th Annual Meeting of the American Society of Gene Therapy, Boston, MA.

Yushkevich, P.A., Piven, J., Hazlett, H.C., Smith, R.G., Ho, S., Gee, J.C., and Gerig, G. (2006). User-guided 3D active contour segmentation of anatomical structures: Significantly improved efficiency and reliability. Neuroimage 31, 1116–1128.

Zhu, X., Hadhazy, M., Wehling, M., Tidball, J.G., and McNally, E.M. (2000). Dominant negative myostatin produces hypertrophy without hyperplasia in muscle. FEBS Lett. 474, 71–75.

Address reprint requests to:
Dr. Xiao Xiao
Division of Molecular Pharmaceutics
University of North Carolina School of Pharmacy
Chapel Hill, NC 27599

E-mail: xxiao@email.unc.edu

Received for publication August 27, 2008;
accepted after revision October 1, 2008.

Published online: January 14, 2009.